EBioMedicine 32 (2018) 182–191

Contents lists available at ScienceDirect

EBioMedicine

journal homepage: www.ebiomedicine.com

Research Paper

By Targeting *Atg7* MicroRNA-143 Mediates Oxidative Stress-Induced Autophagy of c-Kit$^+$ Mouse Cardiac Progenitor Cells

Wenya Ma [a,b,c,1], Fengzhi Ding [a,b,1], Xiuxiu Wang [a,b,1], Qi Huang [a,b], Lai Zhang [a,b], Chongwei Bi [a,b], Bingjie Hua [a,b], Ye Yuan [a,b], Zhenbo Han [a,b], Mengyu Jin [a,b], Tianyi Liu [a,b], Ying Yu [a,b], Benzhi Cai [a,b,c,*,1], Zhimin Du [a,b,c,*,1]

[a] Department of Pharmacy of The Second Affiliated Hospital, Harbin Medical University (Heilongjiang Provincial Key Laboratory of Drug Research, Harbin Medical University), Harbin, China
[b] Department of Pharmacology (Key Laboratoryof Cardiovascular Research, Ministry of Education), College of Pharmacy, Harbin Medical University, Harbin, China
[c] Institute of Clinical Pharmacy, Harbin Medical University, Harbin, China

ARTICLE INFO

Article history:
Received 19 March 2018
Received in revised form 1 May 2018
Accepted 16 May 2018
Available online 30 May 2018

Keywords:
Autophagy
Atg7
Cardiac progenitor cells
MicroRNAs
MI

ABSTRACT

Therapeutic efficiency of cardiac progenitor cells (CPCs) transplantation is limited by its low survival and retention in infarcted myocardium. Autophagy plays a critical role in regulating cell death and apoptosis, but the role of microRNAs (miRNAs) in oxidative stress-induced autophagy of CPCs remains unclear. This study aimed to explore if miRNAs mediate autophagy of c-kit$^+$ CPCs. We found that the silencing of miR-143 promoted the autophagy of c-kit$^+$ CPCs in response to H_2O_2, and the protective effect of miR-143 inhibitor was abrogated by autophagy inhibitor 3-methyladenine (3-MA). Furthermore, autophagy-related gene 7 (*Atg7*) was identified as the target gene of miR-143 by dual luciferase reporter assays. In vivo, after transfection with miR-143 inhibitor, c-kit$^+$ CPCs from green fluorescent protein transgenic mice were more observed in infarcted mouse hearts. Moreover, transplantation of c-kit$^+$ CPCs with miR-143 inhibitor improved cardiac function after myocardial infarction. Take together, our study demonstrated that miR-143 mediates oxidative stress-induced autophagy to enhance the survival of c-kit$^+$ CPCs by targeting *Atg7*, which will provide a complementary approach for improving CPC-based heart repair.

1. Introduction

Ischemic heart disease (IHD) is a leading health problem with high morbidity and mortality. The limited regenerative capacity of adult hearts can't compensate for the lost cardiomyocytes after injury such as myocardial infarction (MI). The enormous loss of cardiomyocytes leads to compromised cardiac function or even heart failure [24]. Recently, cardiac progenitor cells (CPCs) are emerging as a particularly promising approach for heart disease therapy. Lots of reports have demonstrated that CPCs could improve cardiac functions by differentiating into cardiomyocytes and vascular cells, as well as paracrine action [5,18,21]. c-kit$^+$ CPCs transplantation has been demonstrated to alleviate left ventricular (LV) dysfunction in acute and chronic MI to improve the quality of life in animal model [4]. However, the main challenge that CPCs transplantation faced after transplantation is that >90% of transplanted cells will undergo apoptosis, and only <10% CPCs survive in infracted hearts [19].

Oxidative stress is the main reason for the death of c-kit$^+$ CPCs after transplantation. The transplanted c-kit$^+$ CPCs suffer from cell cycle arrest, apoptosis and senescence in response to oxidative stress [1]. Among these, the most predominant form of stem cell death is apoptosis which has been suggested as the key regulatory target for improving the survival of stem cells. Thus, the suppression of CPCs apoptosis will promote the repairment of damaged myocardium after MI. For example, apurinic/apyrimidinic endonuclease/redox factor 1 overexpression inhibited CPCs apoptosis by activating TAK1 and NF-κB signal to promote stem cells survival and improve cardiac functions [2].

Autophagy is a stress adaptation that eliminates aged or damaged cellular components through mechanisms including lysosome-associated digestion. Recent studies showed that autophagy plays an important role in determining the viability and apoptosis of stem cells under oxidative stress. It was found that autophagy induced by H_2O_2 confers stem cells to overcome the apoptosis and enhances its resistance under oxidant stress. Suppression of autophagy exacerbated the apoptosis and reduced the viability of stem cells, and on the contrary,

Abbreviations: Atg7, autophagy-related gene 7; CPCs, cardiac progenitor cells; GFP, green fluorescent protein; LV, left ventricular; MI, myocardial infarction; 3-MA, 3-methyladenine; mRFP, monomeric red fluorescent protein; SQSTM1, sequestosome 1; IHD, ischemic heart disease; LVIDd, left ventricular internal diastolic diameter; LVIDs, left ventricular internal dimension at end-systole; LV vol d, left ventricular end diastolic volume; LV vol s, left ventricular end-systolic volume; EF, ejection fraction; FS, fractional shortening; HE, hematoxylin and eosin.

* Corresponding authors at: Department of Pharmacy of The Second Affiliated Hospital, Harbin Medical University, Harbin 150086, Heilongjiang Province, China.
E-mail addresses: caibz@ems.hrbmu.edu.cn (B. Cai), dzm1956@126.com (Z. Du).
[1] These authors made equal contribution to this work.

https://doi.org/10.1016/j.ebiom.2018.05.021

promoting autophagy may enhance the resistance of stem cells to oxidative stress [27].

MiRNAs play important roles in regulating many cellular events, including cell proliferation, differentiation and apoptosis. For example, miR-17–92 cluster has been shown to induce proliferation of cardiomyocytes [9]. It also has been reported that loss of miR-128 promoted cardiomyocytes proliferation and heart regeneration [14]. MiR-16 and miR-26 overexpression inhibited endothelial cell function [15,20]. MiR-210 inhibited antiangiogenic factors to induce angiogenesis [13]. In addition, miR-199a-3p regulated p53 by targeting CABLES1 in mouse cardiac c-kit$^+$ cells to promote proliferation and inhibit apoptosis through a negative feedback loop [17]. It has been reported that miRNAs are involved in autophagy in some cells including miR-106b, miR-124, miR-143, miR-155 and miR-375, etc. [8,10,12,16,23]. However, the role of miRNAs in the autophagy and apoptosis of CPCs under oxidative stress remains unclear. In this study, we aim to investigate whether miR-143 mediates the autophagy to enhance cellular survival and inhibit apoptosis of transplanted CPCs, and thus improve transplantation efficiency and restore cardiac function after MI.

2. Materials and Methods

2.1. Experimental Animals

The neonatal (1–3 days) mice and 6–8 weeks old male C57BL/6 mice (20–25 g) were purchased from the Experimental Animal Center of The Affiliated Second Hospital of Harbin Medical University (Harbin, China). β-actin driven enhanced green fluorescent protein transgenic mice were purchased from Cyagen (Suzhou, China). The mice were housed in SPF condition. Environmental conditions were a temperature of 21 °C ± 2 °C, humidity of 55% ± 10%. Food and water were freely available throughout the experiments. During housing, animals were monitored twice daily for health status. All mice were randomly assigned to receive different treatments, and the experimenters were blind to treatment condition in this study. All groups were each conducted using 6 animals. All experiments were performed according to the protocols approved by the Institutional Animal Care and Use Committee of Harbin Medical University. The investigation conforms to the *Guide for the Care and Use of Laboratory Animals* published by the US National Institutes of Health (NIH Publication No. 85-23, revised 1985).

2.2. Isolation and Culture of c-Kit$^+$ CPCs

The CPCs were isolated and cultured as described in previous literatures [6,18]. In brief, the hearts from neonatal (1–3 days) mice were minced into 1–2 mm^3 pieces and then incubated for 5 min at 37 °C in 0.25% trypsin (Beyotime) and 0.1% collagenase II (GIBCO, Milan, Italy) alternately for three times. The remaining tissues were collected and cultured in high glucose medium containing 10% fetal bovine serum, 100 U/mL penicillin G and 100 μg/mL streptomycin at 37 °C. Cell generation was performed by 0.25% trypsin, and the third passage of CPCs was used in this study.

2.3. Immunofluorescence

CPCs were washed with PBS, and then fixed with 4% paraformaldehyde for 15 min at 37 °C. Cells were blocked in Normal Goat Serum for 30 min at 37 °C after permeabilized with 0.5% Triton X-100 in PBS for 90 min at room temperature, and then CPCs were incubated with primary antibody LC3 (Sigma-Aldrich Cat# L7543, RRID:AB_796155) overnight. The CPCs were incubated with secondary antibody (EarthOx, San Francisco, CA, USA) and DAPI (Sigma-Aldrich, St. Louis, MO, USA) was used to counterstain the nucleus. The experimenters were blind to group assignment.

2.4. TdT Mediated dUTP Nick End Labelling (TUNEL)

The assay was performed according to the manufacturer's instructions. In brief, the cells were fixed with 4% paraformaldehyde for 15 min at 37 °C, then washed with PBS for three times. Blocking buffer (3% H_2O_2 in CH_3OH) was added to the wells. The cells were incubated in permeabilizing solution (0.1% Triton in 0.1% sodium citrate) after washed with PBS, then added 50uL viaL 1 and 450uL viaL 2 (Roche) and incubated for 1 h at 30 °C. Nucleus counterstained with DAPI for 15 min at room temperature. All participants were blind to treatment assignment.

2.5. Quantitative Real-Time PCR

Total RNA was extracted from CPCs using TRIzol reagent. PCR was performed using GreenER Two-Step qRT-PCR Kit Universal (Invitrogen). The gene-specific primers sequence for miR-143, forward: GCGGCGGG GTGCAGTGCTGCATC, reverse: ATCCAGTGCAGGGTCCGAGG. RT-Primer: GTCGTATCCAGTGCAGGGTCCGAGGTATTCGCACTGGATACGACCCAGAG. The GAPDH was used as control. The experimenters were blind to group assignment.

2.6. Transfection

Diluted inhibitor-NC, miR-143 inhibitor, mimics-NC or miR-143 mimics (Genep-harma, Shanghai, China) were mixed with diluted Opti-MEM® I Reduced Serum Medium (Gibco, New York, NY, USA) and then stand for 20 min. The mixture was used to transfection. MiR-143 mimics: 5′ UGAGAUGAAGCACUGUAGCUC 3′, 5′ GCUACAGUGCUU CAUCUCAUU 3′. MiR-143 inhibitor: GAGCUACAGUGCUUCAUCUCA. ATG7 siRNA: GCUAGAGACGUGACACAUATT, UAUGUGUCACGUCUCU AGCTT.

2.7. Live/Dead Cell Staining

Live/Dead Cell Staining Kit for CPCs survival rate was performed. LIVE/DEAD® fixable dead cell stain was diluted by 50 μL DMSO, and then PBS was used to wash the cells after incubated with diluted stain for 30 min. The experimenters were blind to treatment condition.

2.8. EdU Incorporation Assay

Cell-Light EdU Apollo567 in Vitro Kit (RIBOBIO) was used to detect the proliferation rate according to the manufacturers' instructions. In brief, CPCs were incubated with 5-Ethynyl-2′-deoxyuridine (EdU) for 2 h at 37 °C. Cells were fixed with 4% paraformaldehyde for 15 min at 37 °C. Then Apollo Staining reaction liquid was added into the wells to detect the positive cell. Nucleus counter stained with DAPI for 15 min at room temperature. The experimenters were blind to treatment condition.

2.9. Western Blot

CPCs were split to extract total protein with RIPA lysis Buffer (Thermo Scientific Pierce). BCA assay (Thermo Fisher Scientific) was used to determine the concentration. Proteins were separated by SDS-PAGE, and then transferred from the gel to the Pure Nitrocellulose Blotting membrane (Millipore, Bedford, MA, USA). The membrane was incubated with appropriate primary antibodies at 4 °C overnight and then incubated with secondary antibodies for 1 h at room temperature. The primary antibodies used in this study are as following: LC3 (Sigma-Aldrich Cat# L7543, RRID:AB_796155), C-CASPASE-3 (Cell Signaling Technology Cat# 9654S, RRID:AB_10694088), β-actin (ZSGB-Bio Cat# TA-09, RRID:AB_2636897), SQSTM1 (Cell Signaling Technology Cat# 5114, RRID:AB_10624872), ATG7 (Cell Signaling Technology Cat# 8558, RRID:AB_10831194).

2.10. 3′-UTR Luciferase Construct and Dual Luciferase Reporter Assays

The 3'-UTR of *Atg7* was ligated into the firefly luciferase reporter construct, and HEK293 cells were seeded in 6-well plates and incubated for 24 h. Cells were co-transfected with 3'-UTR reporter plasmids together with miR-143 for 36 h. Renilla luciferase expression plasmid was transfected as control. Dual luciferase reporter assays were used to detect luciferase activities.

2.11. Live-Cell Imaging for Autophagic Flux

The mRFP-GFP-LC3 adenoviral was purchased from HanBio (Shanghai, China). CPCs were infected with adenoviral, and after infection, the cells were cultured for another 72 h. Live Cell Imaging System was used to observe the autophagy flux.

2.12. Construction of Myocardial Infarction Model

Myocardial infarction model was constructed as described previously [3,11]. Briefly, the mice received tracheal intubation and anesthetization with isoflurane containing 3% isoflurane for induction and 2% isoflurane for maintenance. Myocardial infarction was induced by permanent ligation of the left anterior descending coronary artery. Animals that underwent thoracotomy without artery ligation or cell injection were used as sham controls. To prevent wound infection, the iodophor was used to treat wounds twice daily.

2.13. Transplantation of GFP^+ CPCs

At 5 min post ligation, 1×10^5 CPCs from green fluorescent protein transgenic mice transfected with miR-143 inhibitor or NC for 48 h were injected into three sites around infarct border zone. 4 weeks after injection, the mice were sacrificed and the hearts were harvested for immunohistochemistry. Frozen slices of the hearts were immunostained with anti-α-actinin and the nucleus counter stained with DAPI. Arrows indicate eGFP labelled cells.

2.14. Statistical Analyses

Group data are expressed as mean ± SEM with 95% confidence interval. Statistical analysis was performed using two-tailed unpaired Student's *t*-test for comparisons between two groups, or one-way ANOVA followed by Newman-Keuls for comparisons among multiple groups using the GraphPad Prism 5.0 (Graphpad Software, lnc., la Jolla,

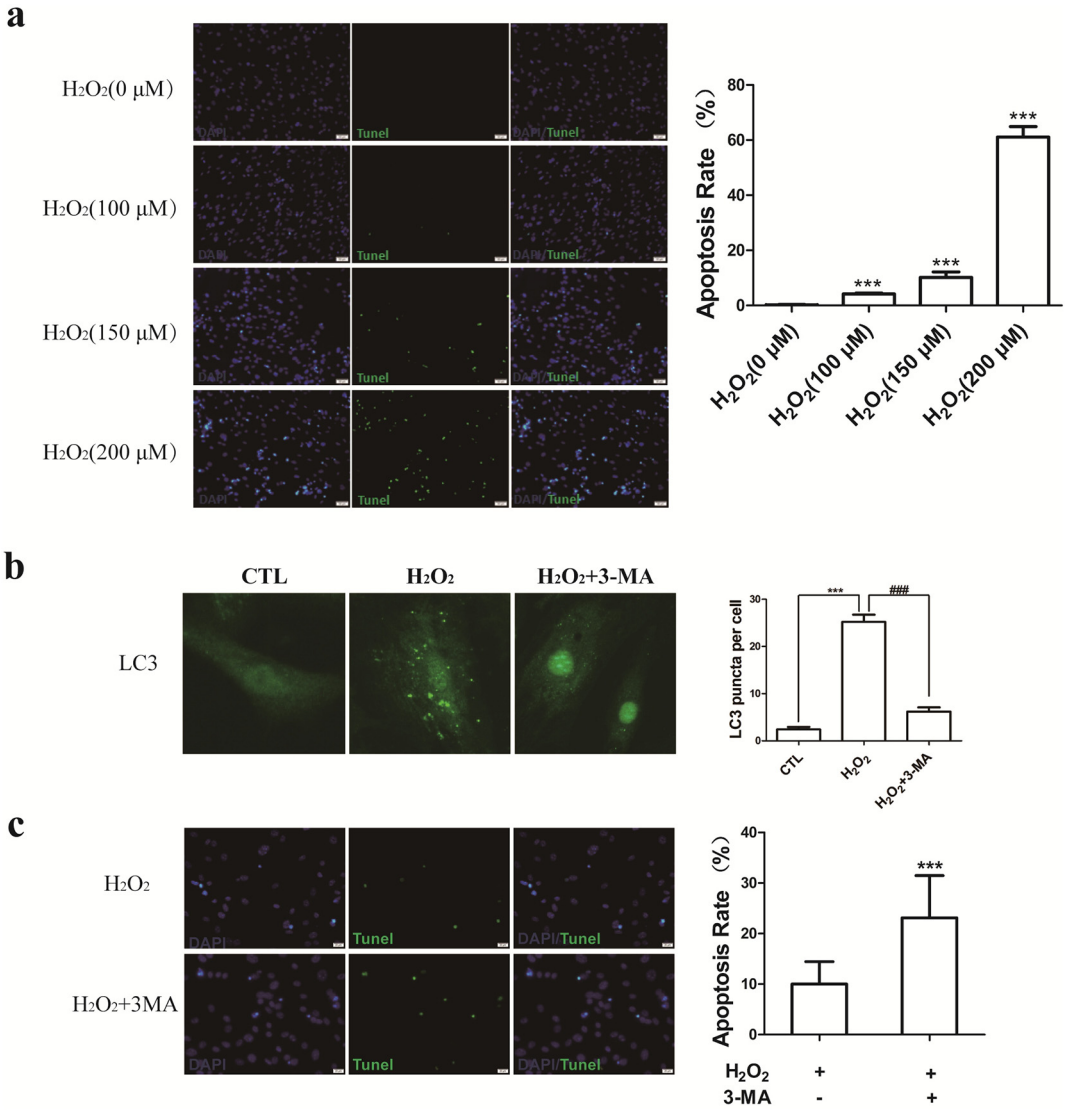

Fig. 1. Involvement of autophagy in H_2O_2-induced apoptosis of CPCs. (a) TUNEL assay for apoptosis of CPCs that were treated with different concentrations of H_2O_2 for 24 h in serum-free media. n ≥ 3, ***P < 0.001 vs. H_2O_2 (0 μM). (b) CPCs were exposed to H_2O_2 150 μM in the presence or absence of 3-MA (5 mM), and then immunostaining showed the localization of LC3. n ≥ 3, ***p < 0.001, ###p < 0.001. (c) TUNEL assay was conducted to detect the apoptosis of CPCs. n ≥ 3, ***p < 0.001 vs. H_2O_2.

California). All data were repeated at least three independent experiments. $P < 0.05$ was considered statistically significant.

3. Results

3.1. Involvement of Autophagy in H_2O_2-Induced Apoptosis of CPCs

We exposed the cultured c-kit$^+$ CPCs to different concentrations of H_2O_2 (0 μM, 100 μM, 150 μM and 200 μM) for 24 h in the serum-free media, and the percentages of apoptotic CPCs significantly increased at the concentration of 150 μM and 200 μM H_2O_2 (Fig. 1a). Thus, in this study, treatment with H_2O_2 150 μM for 24 h in serum-free media was used to induce the damage of CPCs. Moreover, we also observed whether H_2O_2 150 μM induced the autophagy of CPCs. Interestingly, we found that LC3 punctuate structures were increased by H_2O_2 150 μM in CPCs, but autophagy inhibitor 3-methyladenine (3-MA, 5 mM) abrogated the process (Fig. 1b). It indicates that oxidative stress leads to the viability reduction and autophagy induction in CPCs. To determine the impact of H_2O_2-induced autophagy on apoptosis of CPCs, we exposed the cells to H_2O_2 after blocking autophagy using 3-MA, and we found that the cells treated with H_2O_2 in the presence of 3-MA displayed significantly increased apoptosis (Fig. 1c), suggesting that autophagy plays a protective role in H_2O_2-induced apoptosis.

3.2. Effect of miR-143 on Apoptosis and Autophagy of CPCs under Normal Conditions

We further detected the expression of some autophagy-related miRNAs: miR-106b, miR-124, miR-143, miR-155 and miR-375 in H_2O_2-treated CPCs. qRT-PCR confirmed that miR-143 was significantly upregulated by H_2O_2, but miR-124 was significantly downregulated (Fig. 2a). We then investigated whether miR-143 regulates the viability and apoptosis of CPCs under normal conditions. The cultured CPCs were transfected with miR-143 inhibitor (100 nM), inhibitor-NC (100 nM), miR-143 mimics (50 nM) or mimics-NC (50 nM) for 48 h. The data suggest that miR-143 does not regulate the survival, apoptosis and autophagy of CPCs under normal conditions (Fig. 2b-d).

3.3. MiR-143 Mediates Oxidative Stress-Induced Apoptotic Cell Death of CPCs

We further determined the regulatory role of miR-143 in H_2O_2-induced viability reduction and apoptosis of CPCs. The cells were transfected with miR-143 inhibitor, miR-143 mimics or their negative control for 48 h, and incubated with H_2O_2 for 24 h. Live/Dead Cell staining and EdU incorporation assay showed that miR-143 mimics could exacerbate H_2O_2-induced the viability and proliferation reduction of CPCs (Fig. 3a-b). TUNEL staining further demonstrated that forced expression of miR-143 promoted the apoptosis of CPCs in the presence of H_2O_2 (Fig. 3c). On the contrary, knockdown of miR-143 obviously attenuated the viability reduction of CPCs induced by H_2O_2 compared with inhibitor-NC (Fig. 3d). Silencing miR-143 abrogated H_2O_2-induced increase of CPCs apoptosis and decrease of CPCs proliferation (Fig. 3e-f). It suggests that miR-143 inhibitor antagonizes H_2O_2-induced apoptosis of CPCs. Consistently, miR-143 inhibitor attenuated the increased expression of cleaved CASPASE-3 (C-CASPASE-3) induced by H_2O_2 in CPCs, but forced expression of miR-143 enhanced the expression of C-CASPASE-3 (Fig. 3g-h). These data suggest that miR-143 mediates H_2O_2-induced damage of CPCs, and knockdown of miR-143 enhances the resistance of CPCs to oxidative stress.

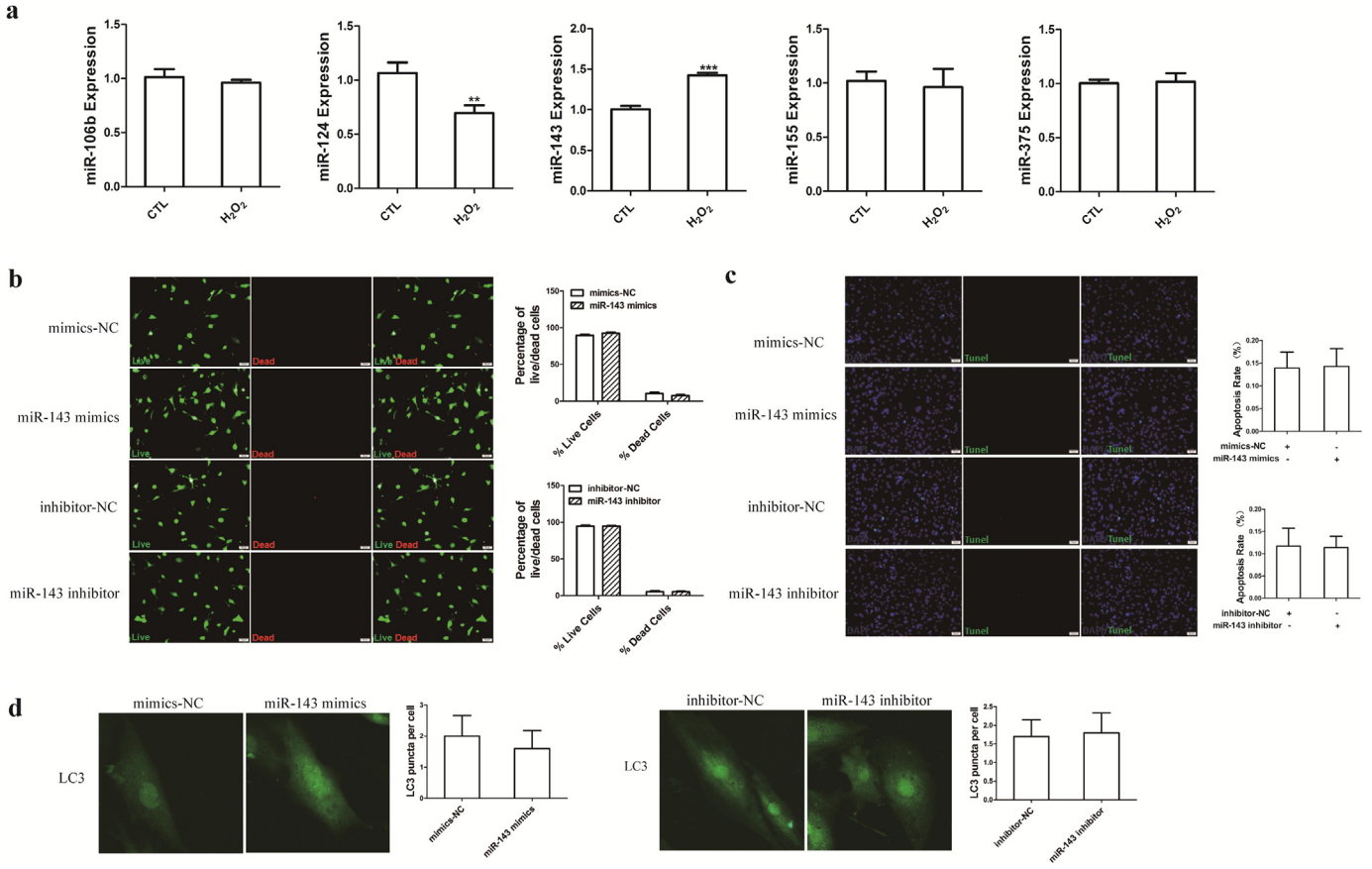

Fig. 2. Effect of miR-143 on apoptosis and autophagy of CPCs under normal conditions. (a) qRT-PCR analysis for the expression of miRNAs in CPCs after treatment with or without H_2O_2 for 24 h in serum-free media. $n \geq 3$, $^{**}p < 0.01$ vs. CTL, $^{***}p < 0.001$ vs. CTL. (b-c) Live/Dead Cell Staining and TUNEL assay were used to detect the rate of survival and apoptosis. (d) Autophagy level was measured by immunostaining of LC3 punctuate structures. $n \geq 3$.

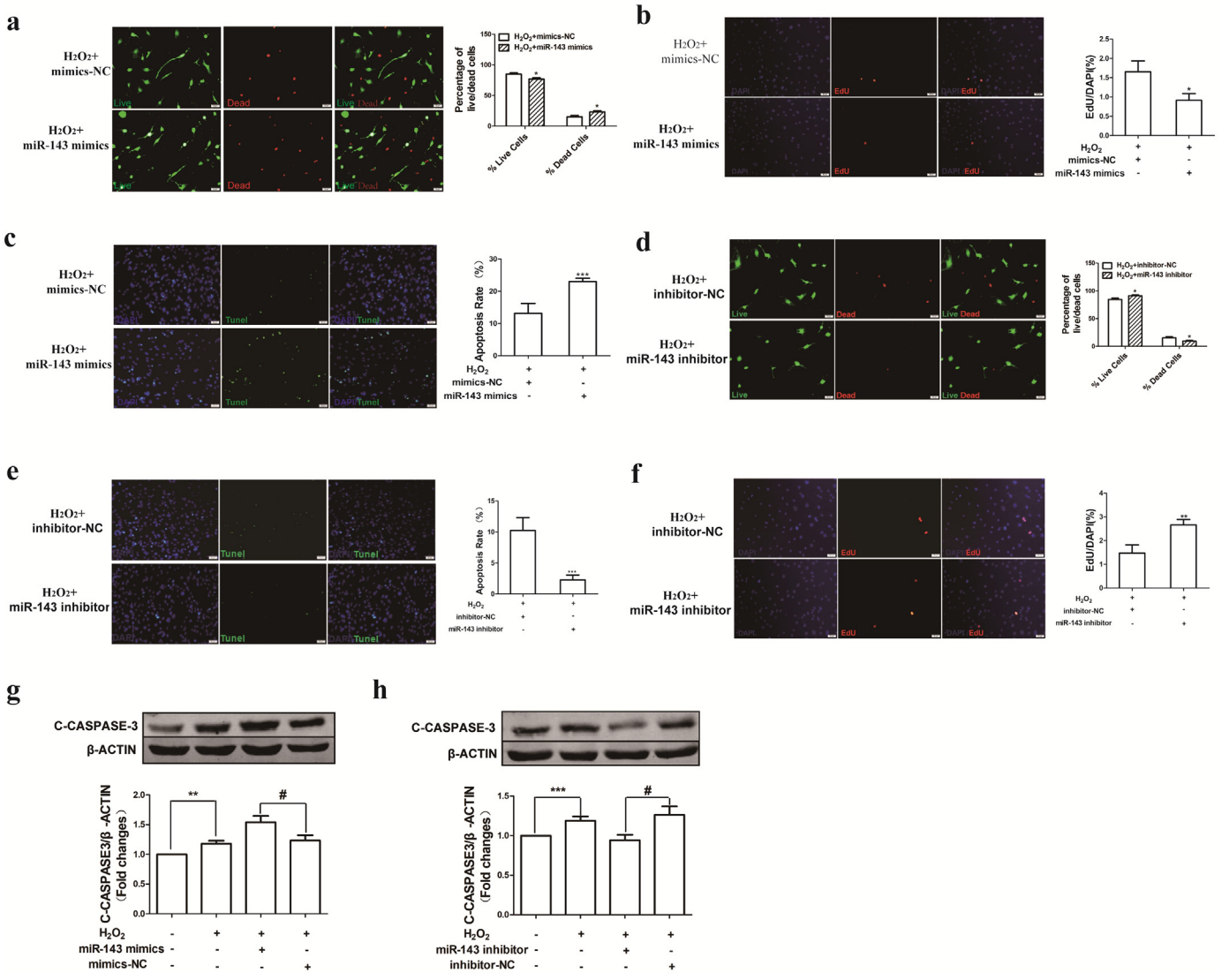

Fig. 3. MiR-143 mediates oxidative stress-induced apoptotic cell death of CPCs. (a) Live/Dead Cell Staining was used to measure the rate of live and dead cells. (b) EdU incorporation assay showed forced expression by miR-143 mimics reduced the proliferative capacity in H_2O_2 treated CPCs. (c) TUNEL assay was used to detect the rate of apoptosis. n ≥ 3, *P < 0.05 vs. H_2O_2 + mimics-NC, ***P < 0.001 vs. H_2O_2 + mimics-NC. (d) Live/Dead Cell Staining was used to measure the rate of live and dead cells. (e) TUNEL assay was used to detect the rate of apoptosis. (f) EdU incorporation assay showed that miR-143 inhibitor increased EdU positive cells. n ≥ 3, *p < 0.05 vs. H_2O_2 + inhibitor-NC, **p < 0.01 vs. H_2O_2 + inhibitor-NC, ***p < 0.001 vs. H_2O_2 + inhibitor-NC. (g-h) Western blot was used to detect the level of C-CASPASE-3. n ≥ 3, **p < 0.01, ***p < 0.001, #p < 0.05.

3.4. MiR-143 Regulates Oxidative Stress-Induced Autophagy in CPCs

MiR-143 mediates biological activities of CPCs under oxidative stress but not normal condition, which indicates that miR-143 targets at the signal pathway involved in oxidative stress. Thus, we examined the impact of miR-143 on H_2O_2-induced autophagy of CPCs. The CPCs were treated with H_2O_2 for 24 h after transfected with miR-143 mimics, miR-143 inhibitor or their negative control, and the autophagy of CPCs was analyzed by immunofluorescence and Western blot. Overexpression of miR-143 inhibited the accumulation of LC3 punctuate structures in CPCs. On the contrary, a significant increase of LC3 punctuate structures was induced by the knockdown of miR-143 in CPCs (Fig. 4a). The autophagy flux was further measured with live-cell imaging using an mRFP-GFP-LC3 reporter construct. The results showed that less mRFP-GFP-LC3 was detected as red and yellow speckles after miR-143 overexpression than mimics-NC, and miR-143 knockdown increased mRFP-GFP-LC3 accumulation (Fig. 4b). Meanwhile, H_2O_2-induced increased conversion of LC3-I to LC3-II in CPCs were significantly reduced after miR-143 mimics transfection in H_2O_2-treated cells and miR-143 inhibitor could increase this conversion (Fig. 4c-d). The accumulation of SQSTM1/p62 (sequestosome 1) was also detected by Western blot. We found that the forced expression of miR-143 could increase the expression of SQSTM1, and the inhibition of miR-143 decreased the level of SQSTM1 (Fig. 4e-f). These results suggest that miR-143 mediates the autophagy in H_2O_2-induced apoptotic CPCs.

3.5. Atg7 Identified as the Target Gene of miR-143

In order to clarify the mechanism underlying miR-143 mediates autophagy of CPCs, bioinformatics analysis shows the binding sites between miR-143 and *Atg7* that is associated with autophagy, and luciferase assay analysis showed that *Atg7* is a target gene of miR-143 (Fig. 5a-b). Thus, we detected the effect of miR-143 on ATG7 expression in the presence of H_2O_2. Western blot showed that the increase of ATG7 expression by H_2O_2 in CPCs was further enhanced by miR-143 knockdown whereas miR-143 mimics induced a reduction of H_2O_2-induced ATG7 expression (Fig. 5c-d). We inhibited miR-143 and *Atg7* together, and found that the downregulation of *Atg7* by *Atg7* siRNA could abrogate miR-143 inhibitor induced the increase of live cells, reduction of apoptotic cells and improvement of proliferative capacity in response

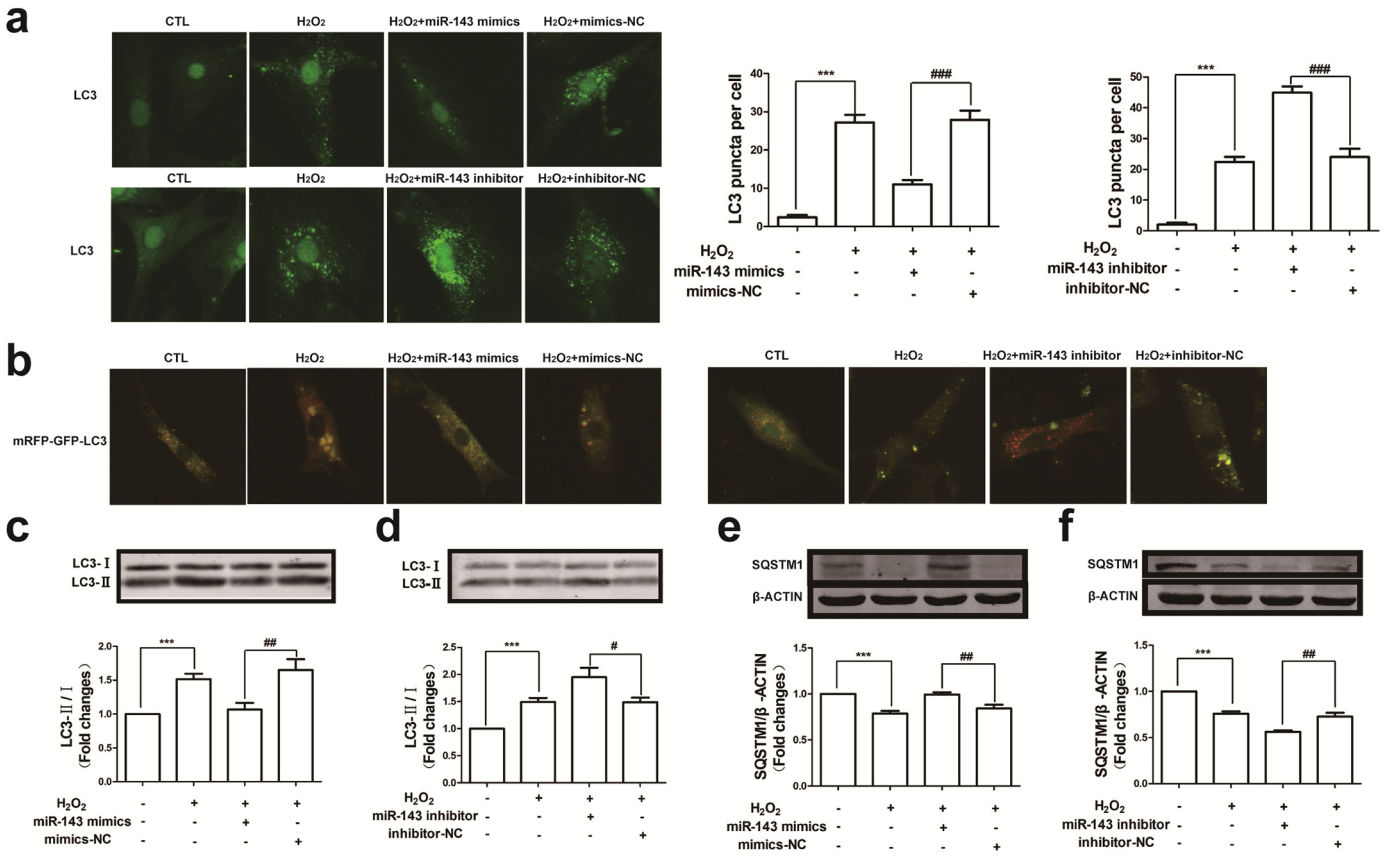

Fig. 4. MiR-143 regulates oxidative stress-induced autophagy in CPCs. (a) Representative images of LC3 punctate in each group. (b) Autophagy flux was also detected by mRFP-GFP-LC3 using Live Cell Imaging Microscopy. The yellow puncta indicate autophagosomes, while red puncta indicate autophagolysosomes. (c-f) Western blot analyzed the conversion of LC3-I to LC3-II and the expression of SQSTM1. n ≥ 3, $^{***}p < 0.001$, $^{\#}p < 0.05$, $^{\#\#}p < 0.01$, $^{\#\#\#}p < 0.001$.

to oxidative stress (Fig. 5e-g). Moreover, we found that *Atg7* knockdown inhibited miR-143 inhibitor induced the increase of conversion of LC3-I to LC3-II and the reduction of SQSTM1 level (Fig. 5h-i). These data suggest that miR-143 impacts the viability and apoptosis of CPCs by targeting *Atg7* to modulate autophagy.

3.6. MiR-143 Silencing Improves Autophagy to Prevent H_2O_2-Mediated CPCs Apoptosis

Many studies have showed that the increase of autophagy is responsible for protective mechanisms in various cells. Therefore, we investigated whether miR-143 influences H_2O_2-induced cell apoptosis via autophagy. The CPCs were treated with H_2O_2 for 24 h after transfection with miR-143 inhibitor or scramble control in the presence of 3-MA. We found that 3-MA could inhibit miR-143 inhibitor-induced accumulation of LC3 punctuate structures, increase of proliferation and reduction of apoptosis in the presence of H_2O_2 (Fig. 6a-c). Consistently, Western blot showed that miR-143 inhibitor-induced conversion of LC3-I to LC3-II and reduction of SQSTM1 were abrogated by 3-MA under oxidative stress condition (Fig. 6d-e). We also used mRFP-GFP-LC3 to detect autophagic flux. Consistently, we found that miR-143 inhibitor-triggered autophagic flux were blocked by 3-MA (Fig. 6f). It indicates that miR-143 inhibitor protects CPCs from H_2O_2-mediated apoptotic damage by regulating autophagy.

3.7. MiR-143 Knockdown Improves Survival of CPCs after Transplantation and Enhances Therapeutic Efficiency in MI

We then further explored whether miR-143 knockdown enhances protective effects of CPCs against myocardial infarction in vivo. CPCs transfected with miR-143 inhibitor for 48 h were injected into the infarcted heart. Four weeks later, echocardiography was performed to evaluate cardiac function. As shown in Fig. 7, echocardiography showed a significant reduced cardiac function in MI model group, but CPCs transplantation showed the improvement of cardiac function after MI, whereas, a more remarkable increase of cardiac function was found in the hearts with transplanted CPCs that transfected with miR-143 inhibitor (Fig. 7a-d). We also found that miR-143 knockdown promoted cardiac morphology and reduced scar size by hematoxylin and eosin (HE)-stain (Fig. 7e). These data suggest that miR-143 knockdown enhances therapeutic efficacy of CPCs transplantation in MI. We further investigated if the improved function is due to increased survival of CPCs through knockdown of miR-143. The cultured CPCs from green fluorescent protein transgenic mice were transfected with miR-143 inhibitor and its corresponding negative control. Then, we transplanted the transfected CPCs into the heart with myocardial infarction by the occlusion of the left coronary artery. As shown in Fig. 7f, we found that the fluorescent cells were more observed in miR-143 knockdown group than in control group. It indicates that miR-143 downregulation may improve the survival rate of CPCs after transplantation.

4. Discussion

Recently, CPCs transplantation is on the rise as an approach for cardiac repair. Previous studies have shown the ability of CPCs to regenerate infarcted myocardium, reconstruct blood vessel and improve cardiac function when delivered intramyocardially or intravascularly [18]. However, stem cell therapy was limited by low cellular survival and persistence in host myocardium. Many researchers make their efforts to overcome this problem. It was revealed that Pim-1 enhanced

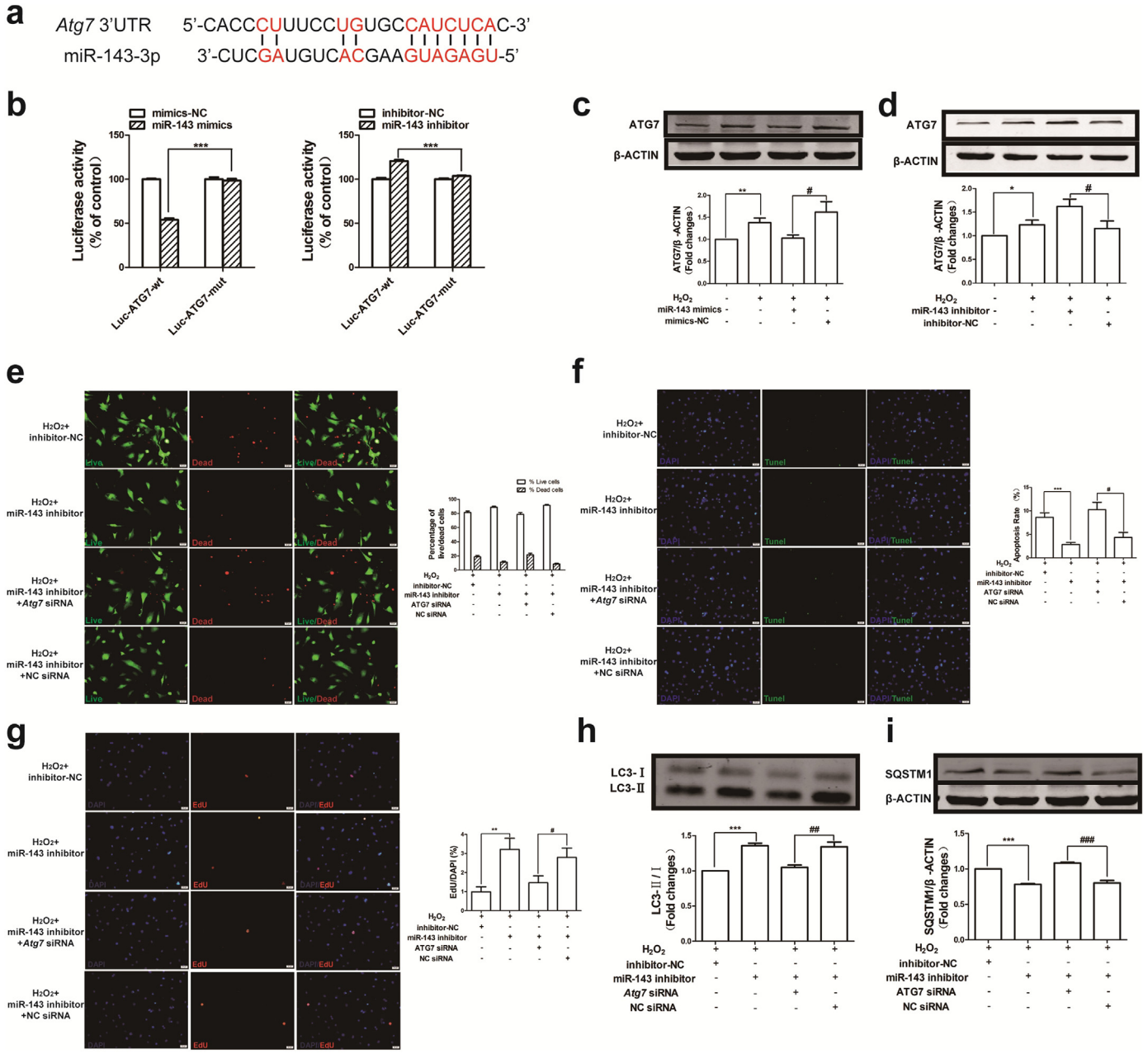

Fig. 5. *Atg7* identified as the target gene of miR-143. (a) The binding site of miR-143 in *Atg7* mRNA. (b) Luciferase reporter assay showed that *Atg7* is the target of miR-143. (c-d) Western blot showing the expression of ATG7 in H_2O_2 150 μM-treated CPCs with miR-143 overexpression or knockdown. (e) Live/Dead Cell staining was used to analyze the survival rate of CPCs after cotransfection with miR-143 inhibitor and *Atg7* siRNA (100 nM). (f-g) Apoptotic CPCs were analyzed by TUNEL assay, and EdU incorporation assay was used to determine the CPCs proliferation. (h-i) Western blot was used to detect the level of LC3 and SQSTM1. n ≥ 3, $^{*}p < 0.05$, $^{**}p < 0.01$, $^{***}p < 0.001$, $^{\#}p < 0.05$, $^{\#\#}p < 0.01$, $^{\#\#\#}p < 0.001$.

the therapeutic effect of CPCs transplantation by increasing the cell proliferation, promoting differentiation of CPCs into cardiac, endothelial, and smooth muscle lineages [11]. In mouse MI model, preconditioning with the heme oxygenase-1 inducer, cobalt protoporphyrin enhanced CPCs survival and improved cardiac function after transplantation [7]. Similarly, diethylemetriamine nitric oxide adduct could also enhance c-kit^{+} CPCs survival by activating multiple cell survival signaling pathways such as STAT3/NFκB and anti-apoptotic signaling pathways [22]. Thus, inhibition of oxidative stress-induced apoptosis of CPCs is a promising strategy for promoting the survival of transplanted CPCs.

In our study, we found that treatment with 150 μM H_2O_2 for 24 h in serum-free media caused a significant increase of cellular apoptosis and autophagy. Interestingly, apoptosis was increased in the presence of 3-MA, indicating that autophagy was involved in the protection of CPCs against apoptosis. Consistently, previous studies have shown that autophagy protected NCI-H460 cells against Calyxin Y induced apoptosis [25]. We also found that the expression of miR-143 was upregulated in CPCs exposed to H_2O_2. Thus, upregulation of miR-143 may be involved in the survival of H_2O_2-treated CPCs. So, what role does miR-143 play in CPCs? We found that miR-143 mimics could promote apoptosis and inhibit proliferation of CPCs in the presence of H_2O_2. On the contrary, miR-143 inhibitor could suppress apoptosis and increase the rate of proliferation in CPCs exposed to H_2O_2. It suggests that miR-143 participates in the process of apoptosis in CPCs.

Interestingly, autophagy contributes to microglial survival that was decreased by administrating methamphetamine while the inhibition of autophagy accelerated the apoptosis as a result of methamphetamine [26]. As described in our study, autophagy level was increased in CPCs after treatment with H_2O_2, and knockdown of miR-143 could enhance autophagy induction and apoptosis reduction. We have demonstrated

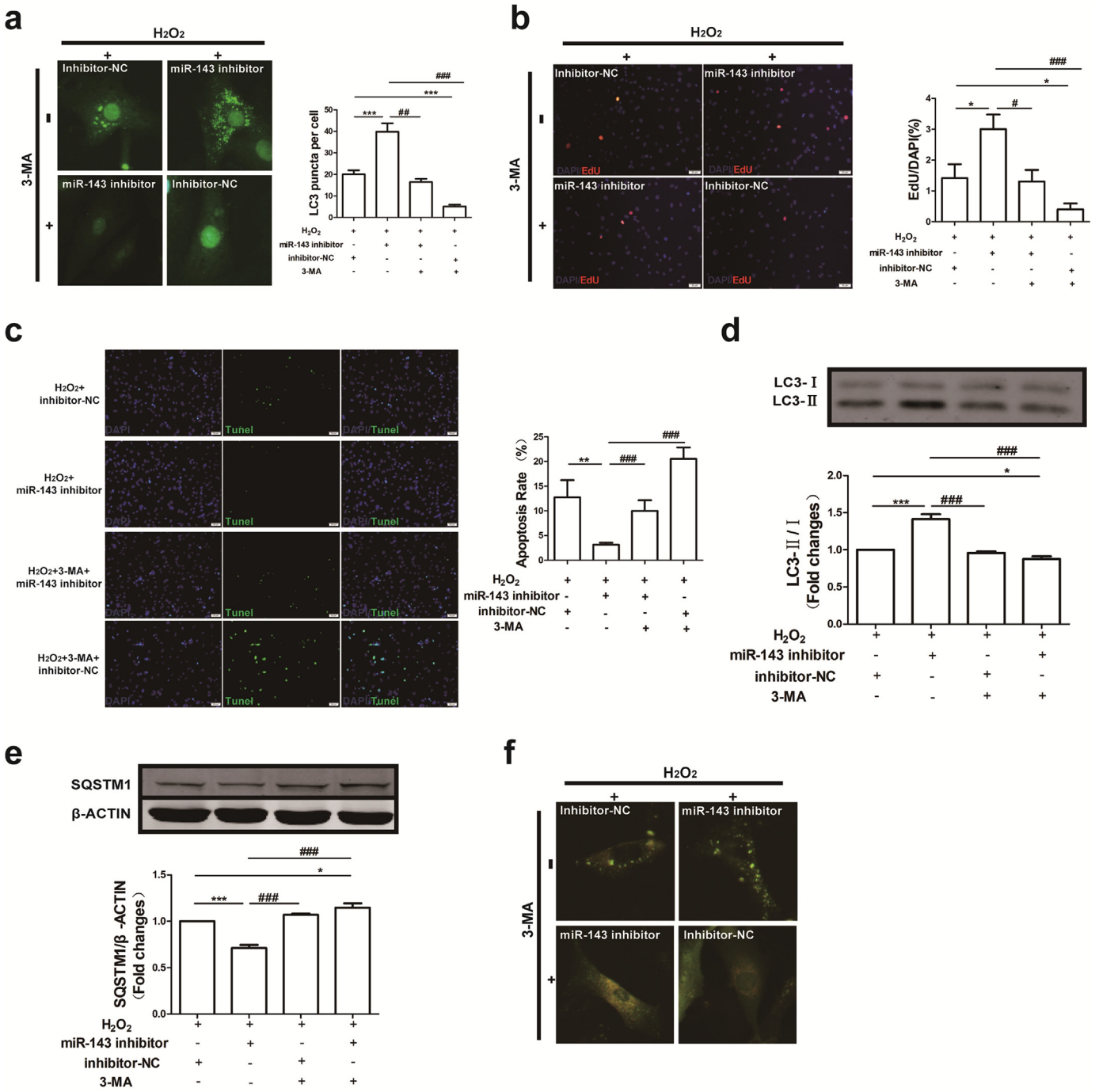

Fig. 6. MiR-143 silencing improves autophagy to prevent H_2O_2-mediated CPCs apoptosis. (a) Immunostaining showing punctate accumulations of LC3 in CPCs after treated with H_2O_2 in the presence or absence of 3-MA. (b) EdU incorporation assay was used to measure the level of CPCs proliferation. (c) TUNEL assay was used to detect the rate of apoptosis. (d-e) Western blot was used to detect the level of LC3 and SQSTM1. (f) Representative images of mRFP-GFP-LC3 in each group. Yellow puncta represent autophagosomes and red puncta represent autolysosomes. n ≥ 3, $^{*}p < 0.05$, $^{**}p < 0.01$, $^{***}p < 0.001$, $^{\#}p < 0.05$, $^{\#\#}p < 0.01$, $^{\#\#\#}p < 0.001$.

Atg7 is a target gene of miR-143, and inhibition of *Atg7* with *Atg7* siRNA could abrogated the protective effect of miR-143 knockdown against oxidative stress.

Interestingly, miR-143′ effects on apoptosis and viability of CPCs were abolished by autophagy inhibitor 3-MA, which indicates that autophagy may be involved in the effect of miR-143 on CPCs survival after transplantation. In vivo study, we found that pre-transfection with miR-143 inhibitor could increase CPCs survival and promote cardiac function. It indicates that the silencing of miR-143 protects CPCs and thus improves cardiac function after CPCs transplantation in MI..

Fig. 7. MiR-143 knockdown improves survival of CPCs after transplantation and enhances therapeutic efficiency in MI. (a-d) MiR-143 inhibitor or inhibitor-NC transfected CPCs were injected into the heart of MI around the ligation point. Cardiac function quantified by left ventricular internal diastolic diameter (LVIDd), left ventricular internal dimension at end-systole (LVIDs), left ventricular end diastolic volume (LV vol d), left ventricular end-systolic volume (LV vol s), ejection fraction (EF) and fractional shortening (FS). (e) Hematoxylin-eosin staining. n ≥ 3, $^{*}p < 0.05$, $^{***}p < 0.001$, $^{\#}p < 0.05$, $^{\#\#}p < 0.01$. $^{\#\#\#}p < 0.001$, $^{\&}p < 0.05$, $^{\&\&}p < 0.01$. (f) CPCs from β-actin driven eGFP transgenic mice transfected with miR-143 inhibitor or inhibitor-NC were used to detect the survival of transplanted CPCs. The white arrows indicate eGFP positive cells.

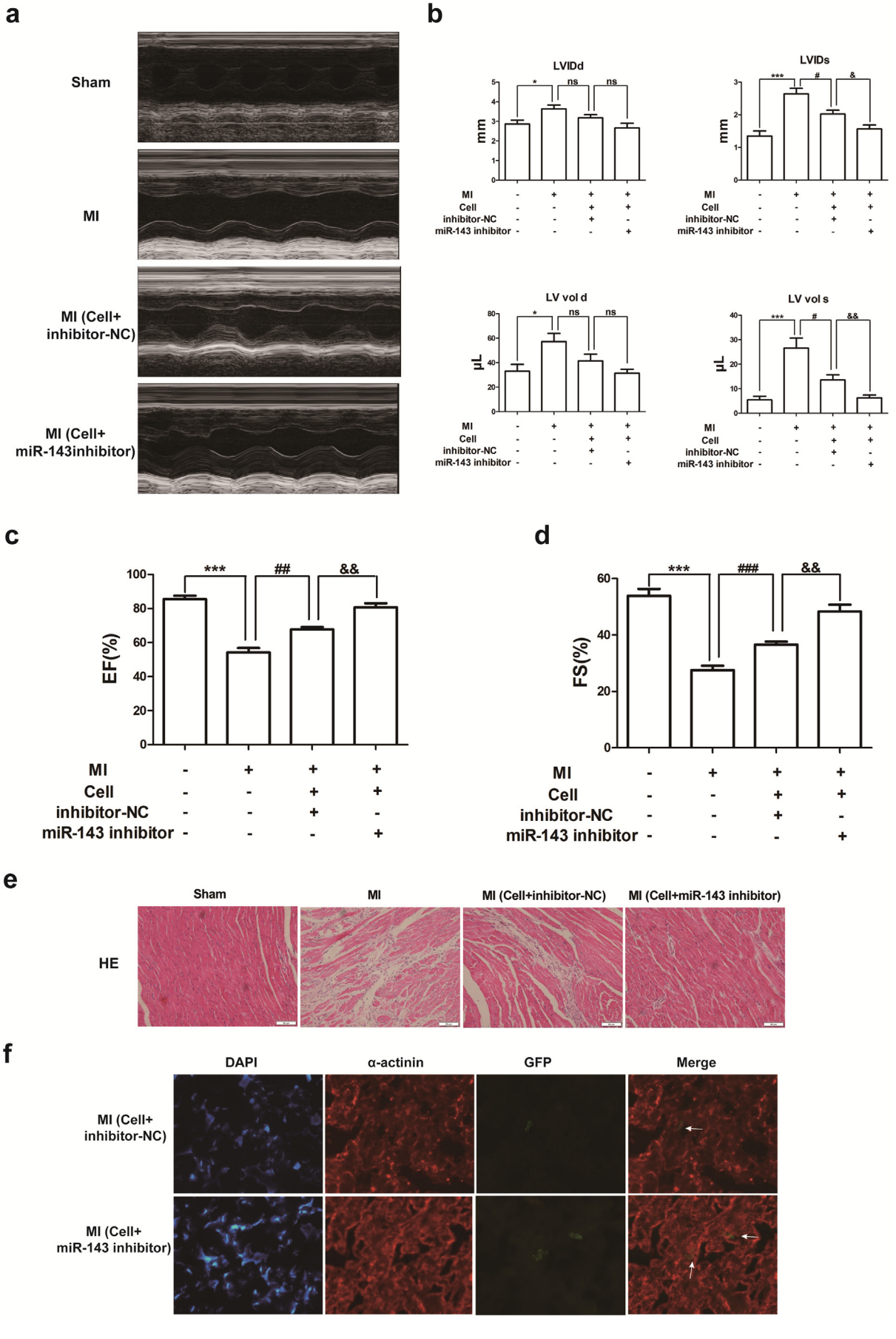
a
Sham
MI
MI (Cell+ inhibitor-NC)
MI (Cell+ miR-143inhibitor)
b
LVIDd
LVIDs
LV vol d
LV vol s
mm
μL
MI
Cell
inhibitor-NC
miR-143 inhibitor
c
EF(%)
d
FS(%)
e
Sham
MI
MI (Cell+inhibitor-NC)
MI (Cell+miR-143 inhibitor)
HE
f
DAPI
α-actinin
GFP
Merge
MI (Cell+ inhibitor-NC)
MI (Cell+ miR-143 inhibitor)

However, miR-143 seems to target more than one autophagy-related gene. Although, we clearly show that miR-143 inhibition improves the survival rate of CPCs under oxidative stress conditions, we did not further conform that this effect was specifically attributed to *Atg7*. We will study the question in the following study. In addition, studies are needed to evaluate therapeutic potential of miR-143 silencing in human cardiac injury. Unfortunately, our study could not contribute to the replacement, refinement or reduction (the 3Rs) of the use of animals in research.

In summary, our findings revealed that miR-143 mediates autophagy of CPCs in response to oxidative stress by targeting *Atg7* and thus regulates the survival of CPCs in MI. It suggests that the silencing of miR-143 will be a potential target for CPCs-based treatment of MI.

Funding Sources

This work was supported by the Major Program of National Natural Science Foundation of China [grant number 81230081], the National Natural Science Fund of China [grant number 81573434, 81170096], and the Program for New Century Excellent Talents In Heilongjiang Provincial University [grant number 1252-NCET-013].

Conflict of Interest

The authors declare no conflicts of interest.

Author Contributions

Benzhi Cai: conception and design, collection and assembly of data and manuscript writing; Wenya Ma, Fengzhi Ding: acquisition, analysis and interpretation of data and manuscript writing; Xiuxiu Wang, Qi Huang, Lai Zhang, Chongwei Bi, Bingjie Hua, Ye Yuan, Zhenbo Han, Mengyu Jin, Tianyi Liu, Ying Yu: acquisition of data; Zhimin Du: conception and design and final approval of manuscript. Wenya Ma, Fengzhi Ding and Xiuxiu Wang contributed equally to this article.

Appendix A. Supplementary data

Supplementary data to this article can be found online at https://doi.org/10.1016/j.ebiom.2018.05.021.

References

[1] Abdelwahid E, Kalvelyte A, Stulpinas A, de Carvalho KA, Guarita-Souza LC, Foldes G. Stem cell death and survival in heart regeneration and repair. Apoptosis 2016;21:252–68.
[2] Aonuma T, Takehara N, Maruyama K, Kabara M, Matsuki M, Yamauchi A, et al. Apoptosis-resistant cardiac progenitor cells modified with apurinic/apyrimidinic endonuclease/redox factor 1 gene overexpression regulate cardiac repair after myocardial infarction. Stem Cells Transl Med 2016;5:1067–78.
[3] Arminan A, Gandia C, Garcia-Verdugo JM, Lledo E, Trigueros C, Ruiz-Sauri A, et al. Mesenchymal stem cells provide better results than hematopoietic precursors for the treatment of myocardial infarction. J Am Coll Cardiol 2010;55:2244–53.
[4] Bolli R, Tang XL, Sanganalmath SK, Rimoldi O, Mosna F, Abdel-Latif A, et al. Intracoronary delivery of autologous cardiac stem cells improves cardiac function in a porcine model of chronic ischemic cardiomyopathy. Circulation 2013;128:122–31.
[5] Breckwoldt K, Weinberger F, Eschenhagen T. Heart regeneration. Biochim Biophys Acta 2016;1863:1749–59.
[6] Cai B, Ma W, Bi C, Yang F, Zhang L, Han Z, et al. Long noncoding RNA H19 mediates melatonin inhibition of premature senescence of c-kit(+) cardiac progenitor cells by promoting miR-675. J Pineal Res 2016;61:82–95.
[7] Cai C, Guo Y, Teng L, Nong Y, Tan M, Book MJ, et al. Preconditioning human cardiac stem cells with an HO-1 inducer exerts beneficial effects after cell transplantation in the infarcted murine heart. Stem Cells 2015;33:3596–607.
[8] Chang Y, Yan W, He X, Zhang L, Li C, Huang H, et al. miR-375 inhibits autophagy and reduces viability of hepatocellular carcinoma cells under hypoxic conditions. Gastroenterology 2012;143:177–87.
[9] Chen J, Huang ZP, Seok HY, Ding J, Kataoka M, Zhang Z, et al. Mir-17-92 cluster is required for and sufficient to induce cardiomyocyte proliferation in postnatal and adult hearts. Circ Res 2013;112:1557–66.
[10] D'Adamo S, Alvarez-Garcia O, Muramatsu Y, Flamigni F, Lotz MK. MicroRNA-155 suppresses autophagy in chondrocytes by modulating expression of autophagy proteins. Osteoarthritis Cartilage 2016;24:1082–91.
[11] Fischer KM, Cottage CT, wu W, Din S, Gude NA, Avitabile D, et al. Enhancement of myocardial regeneration through genetic engineering of cardiac progenitor cells expressing Pim-1 kinase. Circulation 2009;120:2077–87.
[12] Gong X, Wang H, Ye Y, Shu Y, Deng Y, He X, et al. miR-124 regulates cell apoptosis and autophagy in dopaminergic neurons and protects them by regulating AMPK/mTOR pathway in Parkinson's disease. Am J Transl Res 2016;8:2127–37.
[13] Hu S, Huang M, Li Z, Jia F, Ghosh Z, Lijkwan MA, et al. MicroRNA-210 as a novel therapy for treatment of ischemic heart disease. Circulation 2010;122:S124–31.
[14] Huang W, Feng Y, Liang J, Yu H, Wang C, Wang B, et al. Loss of microRNA-128 promotes cardiomyocyte proliferation and heart regeneration. Nat Commun 2018;9:700.
[15] Icli B, Wara AK, Moslehi J, Sun X, Plovie E, Cahill M, et al. MicroRNA-26a regulates pathological and physiological angiogenesis by targeting BMP/SMAD1 signaling. Circ Res 2013;113:1231–41.
[16] Liu J, Li M, Wang Y, Luo J. Curcumin sensitizes prostate cancer cells to radiation partly via epigenetic activation of miR-143 and miR-143 mediated autophagy inhibition. J Drug Target 2017;25:645–52.
[17] Liu J, Wang Y, Cui J, Sun M, Pu Z, Wang C, et al. miR199a-3p regulates P53 by targeting CABLES1 in mouse cardiac c-kit(+) cells to promote proliferation and inhibit apoptosis through a negative feedback loop. Stem Cell Res Ther 2017;8:127.
[18] Messina E, de Angelis L, Frati G, Morrone S, Chimenti S, Fiordaliso F, et al. Isolation and expansion of adult cardiac stem cells from human and murine heart. Circ Res 2004;95:911–21.
[19] Muller-Ehmsen J, Whittaker P, Kloner RA, Dow JS, Sakoda T, Long TI, et al. Survival and development of neonatal rat cardiomyocytes transplanted into adult myocardium. J Mol Cell Cardiol 2002;34:107–16.
[20] Spinetti G, Fortunato O, Caporali A, Shantikumar S, Marchetti M, Meloni M, et al. MicroRNA-15a and microRNA-16 impair human circulating proangiogenic cell functions and are increased in the proangiogenic cells and serum of patients with critical limb ischemia. Circ Res 2013;112:335–46.
[21] Tang XL, Li Q, Rokosh G, Sanganalmath SK, Chen N, Ou Q, et al. Long-term outcome of administration of c-kit(POS) cardiac progenitor cells after acute myocardial infarction: transplanted cells do not become cardiomyocytes, but structural and functional improvement and proliferation of endogenous cells persist for at least one year. Circ Res 2016;118:1091–105.
[22] Teng L, Bennett E, Cai C. Preconditioning c-kit-positive human cardiac stem cells with a nitric oxide donor enhances cell survival through activation of survival signaling pathways. J Biol Chem 2016;291:9733–47.
[23] Wu H, Wang F, Hu S, Yin C, Li X, Zhao S, et al. MiR-20a and miR-106b negatively regulate autophagy induced by leucine deprivation via suppression of ULK1 expression in C2C12 myoblasts. Cell Signal 2012;24:2179–86.
[24] Zangi L, Lui KO, Von Gise A, Ma Q, Ebina W, Ptaszek LM, et al. Modified mRNA directs the fate of heart progenitor cells and induces vascular regeneration after myocardial infarction. Nat Biotechnol 2013;31:898–907.
[25] Zhang C, Yang L, Wang XB, Wang JS, Geng YD, Yang CS, et al. Calyxin Y induces hydrogen peroxide-dependent autophagy and apoptosis via JNK activation in human non-small cell lung cancer NCI-H460 cells. Cancer Lett 2013;340:51–62.
[26] Zhang Y, Shen K, Bai Y, Lv X, Huang R, Zhang W, et al. Mir143-BBC3 cascade reduces microglial survival via interplay between apoptosis and autophagy: implications for methamphetamine-mediated neurotoxicity. Autophagy 2016;12:1538–59.
[27] Zhang Z, Yang C, Shen M, Yang M, Jin Z, Ding L, et al. Autophagy mediates the beneficial effect of hypoxic preconditioning on bone marrow mesenchymal stem cells for the therapy of myocardial infarction. Stem Cell Res Ther 2017;8:89.